J. Membrane Biol. 57, 213–221 (1980)

The Journal of
Membrane Biology

Membrane Current and Noise Measurements in Voltage-Clamped Node of *Ranvier*

Rutgeris J. van den Berg* and Willem H. Rijnsburger**

Laboratory of Physiology and Physiological Physics, Leiden, The Netherlands

Summary. In voltage-clamp configurations for nodes of *Ranvier* the axoplasm resistance functions as a voltage-current converter. In existing configurations this resistance cannot be measured directly. In the present arrangement the electrical resistances of the preparation (axoplasm, membrane and seals) can be measured only from two measurements. This allows us to: 1. calibrate the ionic current under voltage-clamp conditions, and 2. calculate the intensity of the current fluctuations, not arising from the membrane (background noise). The measured axoplasm resistances are considerably higher than the values calculated on the basis of fiber geometry and axoplasm resistivity. The difference is due to the presence of constrictions in the nerve fiber. Membrane current estimation based on geometrical parameters in the presence of wide seals may contain large errors. Variations in the axoplasm resistance for voltage-membrane current conversion were observed within 1.5 hr. In 68 % of the fibers this resistance decreased with 30 % of the original value. With our current calibration the values for the maximum sodium conductance $\overline{g_{Na}}$ (at 0 mV membrane potential), maximum potassium conductance $\overline{g_K}$ and leakage conductance $\overline{g_L}$ are 49.5×10^{-8}, 6.66×10^{-8} and 1.71×10^{-8} S, respectively. The contribution of the different noise sources to the total background noise was calculated at the holding potential. For frequencies below 10^3 Hz there is an excellent agreement between measured and calculated noise levels.

Present voltage-clamping techniques for nodes of *Ranvier* are based on the two-amplifier configuration of Dodge and Frankenhaeuser (1958) or the one-amplifier version of Nonner (1969). In these arrangements the quantity of interest, the membrane current, equals e/Z, where e is the output voltage of the clamp-amplifier and Z the impedance of the membrane current-passing path (axoplasm). Since Z is an unknown quantity the magnitude of the membrane current remains unknown. The measurement of Z is precluded by a shunt resistance, formed by the outer surface of the current-passing pathway.

At present, different approaches to determine the membrane current in voltage clamps for *Ranvier* nodes exist:

1. Calculation by Means of an Arbitrarily Chosen Factor (Dodge & Frankenhaeuser, 1958)

To calculate a scale for the membrane current density, which is given by:

$$I = \frac{e}{A\,Z} \tag{1}$$

where A is the nodal membrane area, the authors assumed the product $A \cdot Z$ to be equal to $10\,\Omega\,\mathrm{cm}^2$. This factor was arbitrarily chosen on the basis of probable values for fiber geometry and internodal resistance.

2. Calculation of Z by Means of a Measured Resistance Ratio and an Assumed Resistance Value (Dodge, 1963; Hille, 1971)

To obtain an estimate for Z, the ratio between negative membrane potential changes and the corresponding output voltages of the clamp amplifier are measured. This potential ratio equals the ratio between membrane impedance and Z. Under the assumption

* *Address for reprint requests:* Laboratory of Physiology and Physiological Physics, Wassenaarseweg 62, 2300 RC Leiden, The Netherlands.

** *Present address:* Department of Cardiology, Experimental Cardiology Center, Rijnsburgerweg 10, Leiden, The Netherlands.

0022-2631/80/0057-0213 $01.80

that the membrane impedance equals 40 MΩ in normal Ringer's solution (Tasaki, 1955), Z can be calculated.

3. Calculation of Z Based on Optically Measured Fiber Geometry (Nonner, Rojas & Stämpfli, 1975)

The membrane current can be deduced after calculation of the resistance of the axoplasm, obtained from the geometrical parameters of the fiber measured at the end of an experiment. The longitudinal resistance of the current-passing axoplasm cylinder was calculated from the relation:

$$R = \frac{4\rho l}{\pi \phi_i^2} \tag{2}$$

where ρ is the specific resistance of the axoplasm taken as 110 Ωcm (Huxley & Stämpfli, 1951), l is the length of the cut internode and ϕ_i the internal diameter of the axoplasm.

4. Indirect Determination of Z from Four Independent Measurements (Sigworth, 1980)

Since Z can be regarded as one branch of a four-terminal electrical network, an adequate number of electrical measurements may lead to the solution of a corresponding number of network equations. By suitable application of voltage and current sources at the network terminals, four equations with four unknown resistances can be obtained.

5. Indirect Determination of Z from Three Independent Measurements (Chiu, Ritchie, Rogart & Stagg, 1979)

By zeroing the resistance of one branch of the network (by electrical destruction of the node) reduction to three equations and three unknown resistances is possible.

6. Indirect Determination of Z from Two Measurements (This Paper)

The application of a guarding technique, explained hereafter, which eliminates the shunt current along the outer surface of the nerve fiber, enables us to obtain two equations and two unknown resistances (Z and the membrane resistance). By switching off the electrical guarding, the outer surface shunt resistances can also be determined. The results of these measurements are given in this paper and compared with previously published approaches.

Membrane current fluctuations are contaminated with noise not arising from the nodal membrane. This part of the noise is called background noise and originates from the nerve fiber preparation and the amplifier system. The measurement of the electrical resistances of the nerve fiber preparation allows us to determine the contribution of different noise sources.

Materials and Methods

Arrangement

Single motor fibers of the frog *Rana esculenta* were dissected after the technique described by Stämpfli (1969) at a temperature of 5–10 °C. The isolated fiber was mounted on the nerve chamber, made of one piece of macrolon (Bayer-AG, 5.4 × 3.4 × 1.0 cm). In its surface five pools have been milled (Fig. 1*a*). From the left- to the right-hand side of the preparation these pools are called the *C*, *B*, *A*, *F* and *E* pool, after the original nomenclature of Dodge and Frankenhaeuser (1958). Pool *F* is an extension of this nomenclature, not present in their arrangement. The width of th *B*, *A* and *F* pool are 228, 235, and 215 µm and are 0.9, 2.7 and 0.5 mm deep. The partitions between the pools *CB*, *BA*, *AF*, and *FE* are 480, 114, 118, and 200 µm wide and were all covered with silicone grease. After replacement of the Ringer's solution[1] in pools *C* and *E* by 120 mM KCl, the nerve trunks were cut from the fiber as close as possible to the partition walls (100–200 µm). Between pools *C* and *B* an additional oil gap (Unisilcon oil, TK 003/15000) was made. The oil gap was preceded in time by an air gap, lasting about 30 sec. This procedure proved to be essential to obtain a high electrical resistance (≥ 50 MΩ) but does not guarantee such a value (*cf.* Table 2).

The 5 Ag – AgCl – Pt electrodes (101 H, Annex Research) with KCl-agar bridges are mounted close to the input amplifiers. The nerve chamber has a fixed position and the amplifier housing together with the electrodes can be moved up and down. In this way the electrodes can be immersed in the corresponding pools.

Through pool *A* a constant flow of solution of 1 ml/min is made by a constant fluid level difference between this pool and a chamber with a float. The fluid level in the pool is kept constant by means of a suction device.

The temperature in pool *A* is measured with a thermistor near the node of *Ranvier* (11 mm) and is kept constant (within 0.3 °C) by a feedback system.

The geometry of the preparation was measured at the end of each experiment with a light microscope, sometimes under water immersion, while the fiber was still in the chamber. Diameters were measured in each pool at 1 or 2 positions. In one internode the relative diameter variations were about 10 %; along the whole fiber they were always smaller than 20 %.

The electrical circuit is shown in Fig. 1*b*. Pool *A* is kept at ground potential to achieve a symmetrical electronic arrangement. The noninverting preamplifiers 1 (Analog-Devices 149) and 2 (Teledyne 1025) have a gain of 10. Capacitance neutralization is

[1] The standard Ringer's solution has the following composition (in mM): 115 NaCl, 2.50 KCl, 2.00 $CaCl_2$, 0.50 $MgCl_2$, 5.00 Tris; pH 7.4.

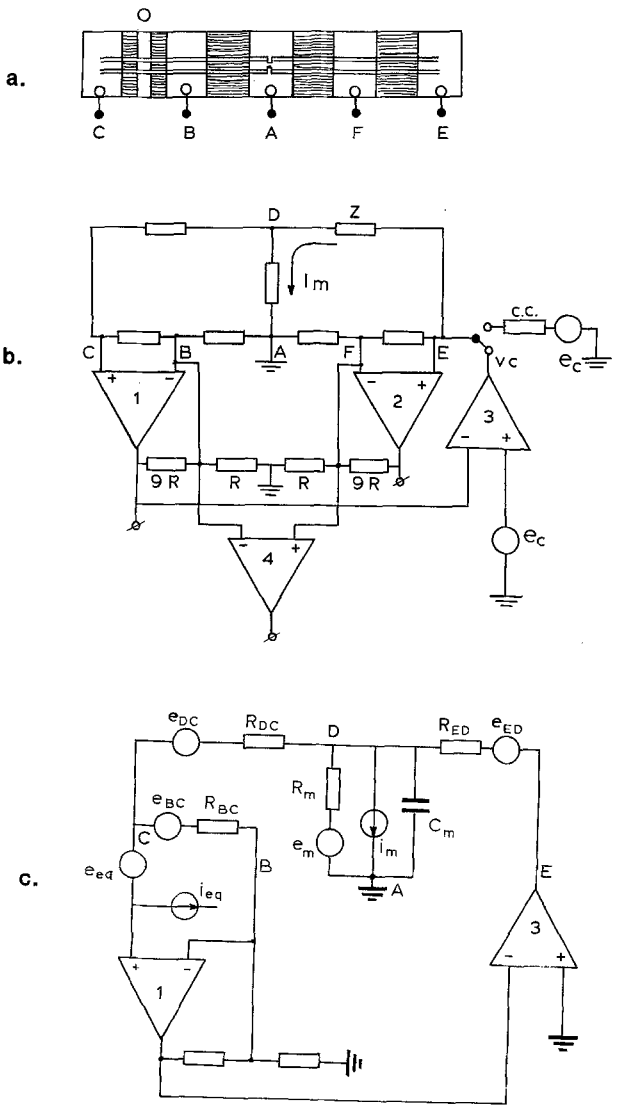

Fig. 1. (*a*) Schematic representation of the fiber on the nerve chamber. *A*, *B*, *C*, *E* and *F* are five saline pools, connected with electrodes to the amplifier system. Pool *0* contains silicone oil. The shaded regions are partitions covered with silicone grease. (*b*) Simplified equivalent circuit of the voltage- and current-clamp arrangement. Feedback isolation amplifiers 1 and 2, voltage-clamp amplifier 3 and current-measuring amplifier 4; e_c is the command potential. (*c*) Noise sources in the voltage-clamp situation. All irrelevant network elements with respect to noise analysis are omitted. The noise current i_m represents the excess membrane noise. The other noise sources are the equivalent sources added to each passive impedance of the preparation and to the amplifier

achieved by the feedback of a variable part of the output voltages of the preamplifiers to the input terminals via a capacitor. Electrical feedback isolation is performed by the incorporation of pool *B* and pool *F* in the negative feedback loops of amplifier 1 and amplifier 2, respectively. This prevents the external flow of current along the preparation between *C* and *B* and between *E* and *F* (Moore & Del Castillo, 1959; Derksen, 1965).

When a current source is connected to pool *E*, this current will flow through axoplasm part *ED* to the nodal membrane (current clamp). Membrane voltage is measured with amplifier 1.

The voltage-clamp situation is achieved by clamp amplifier 3 (Teledyne 1030), where the amplified membrane potential is compared with a command voltage e_c.[2] The clamp amplifier adjusts its output voltage in pool *E* in such a way that the output of amplifier 1 equals the command voltage. The clamp amplifier has a low frequency gain of 500, while a phase-lead network adjusts the high frequency behavior. A small readjustment of the capacitance neutralization of amplifier 1 may sometimes be necessary to obtain a damped response, with a stabilization time of the current between 30–100 μsec (Fig. 2*a* and *b*).

The output voltage of amplifier 4 (Analog-Devices 509-J) equals the voltage difference between the pools *F* and *B*, and thus between pools *E* and *D* which corresponds to $I_m Z$. Since *Z* can be measured (*see* Resistance Measurements), I_m is a known quantity.

Ionic Current Parameter Determination

At the beginning of an experiment the membrane voltage is clamped to a potential, where the Hodgkin-Huxley-parameter $h_\infty = 0.7$, as revealed by the amplitude-ratio of the maximum peak sodium currents, obtained without and with a prepulse of −100 mV for a duration of 40 msec. The leakage currents in the node were measured with 5 to 10 voltage pulses in the range from −100 to −200 mV for a duration of 2 msec. In this voltage range the leakage current is linearly related to the membrane voltage (Dodge, 1963). From the relation

$$i_L = \bar{g}_L (E - E_L) \tag{3}$$

$\bar{g}_L$ and E_L were calculated. To obtain the potassium current parameters five pulses from +50 to +100 mV were given to the membrane for a duration of 20 msec. These pulses were preceded by a prepulse of −90 mV for 2.5 sec to remove potassium inactivation at the holding potential. The isochronic membrane current-voltage relation (at $t = 20$ msec) is linear (Dodge, 1963; Van den Berg, 1978). After subtraction of the calculated leakage current, the potassium current parameters $\bar{g}_K$ and E_K were calculated from:

$$i_K = \bar{g}_K (E - E_K). \tag{4}$$

Resistance Measurements

Via small capacitors (0.2 pF) current pulses are supplied to the *C* and *E* pools. The input capacitance of amplifiers 1 and 2 are neutralized until the step-responses are critically damped. The current pulses are calibrated by switching to a standard resistor (50.6 MΩ).

From the measurement of the voltage responses on these pulses the electrical resistances of the nerve fiber preparation are calculated:[3] axoplasm resistances R_{DC} and R_{ED}, shunt resistances of the seals R_{BC} and R_{EF}, and the membrane resistance R_m. These five quantities can be measured by four consecutive current pulses in the *C* or in the *E* pool and by alternately incorporating the *B* pool and *F* pool in the feedback loop of the preamplifiers. When the feedback is switched off, the corresponding feedback pool is grounded.

[2] This voltage-clamp arrangement resembles the Dodge-Frankenhaeuser configuration (Dodge & Frankenhaeuser, 1958). In the present arrangement pool *A* is at ground potential instead of pool *B*.

[3] The relative error in the resistance measurement is determined by the read-off error from the oscilloscope (3.5 %).

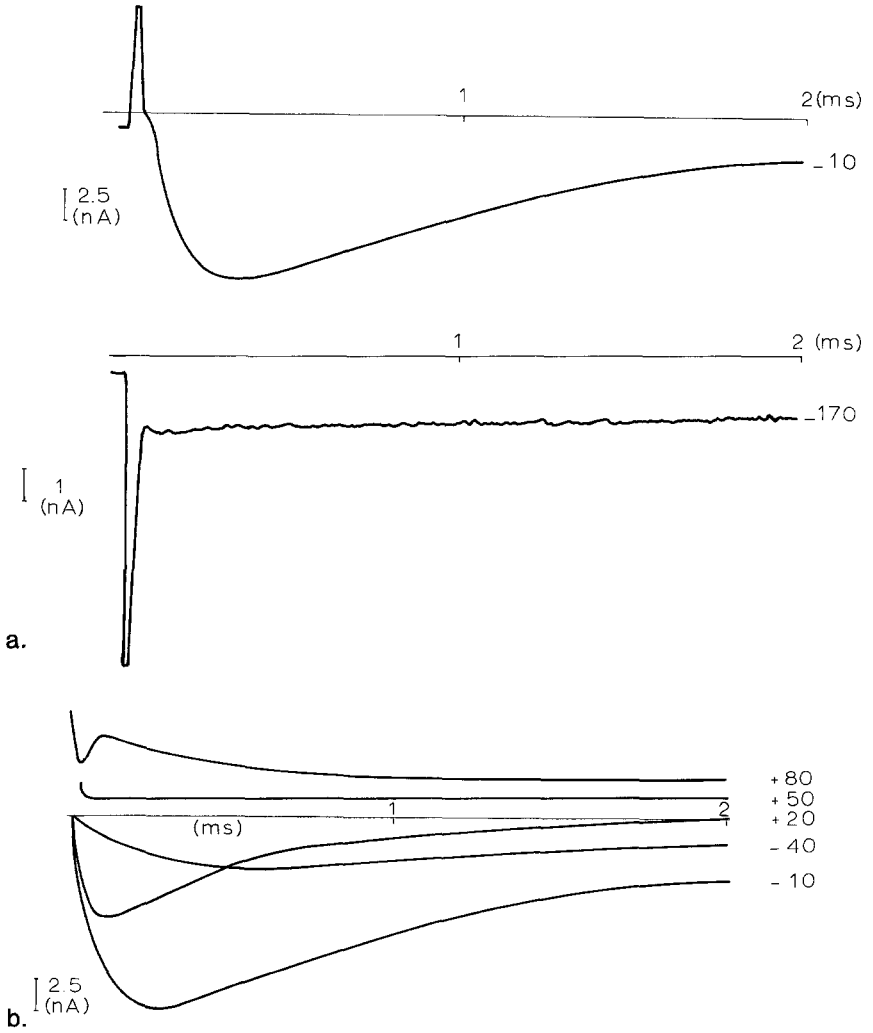

Fig. 2. (*a*) *Upper curve:* Membrane current in response to a voltage step to −10 mV from a prepulse level of −90 mV with a duration of 40 msec (node 771117; parameters in Table 4). *Lower curve:* Capacity and leakage current at a voltage step to −170 mV with a prepulse as in upper curve which has the same voltage step of 80 mV. The duration of the capacity current is about 40 µsec. Membrane currents are the filtered output voltages of amplifier 4 (6-pole Bessel, low-pass, cutoff frequency: 20 kHz) and stored by a transient recorder (Biomation 802). The capacity current peak is outside the scale.
(*b*) Membrane currents in response to step changes in voltage in the presence of 10 mM TEA. Holding potential: −78 mV; prepulse to −90 mV for 40 msec and test voltages (mV) as indicated. Currents shown after 40 µsec. Only at the largest steps of 140 and 170 mV is the capacity current tail seen

Membrane Current Fluctuations

The fluctuations of the output voltage of amplifier 4 correspond to the membrane current fluctuations, but are contaminated with noise from axoplasm, seals and amplifiers (background noise). In Fig. 1*c* a simplified equivalent circuit of the voltage-clamp configuration is shown. Solving the loop equations and assuming infinite amplifier gains the contribution of each noise source can be calculated. The result of this analysis is identical to that given by Conti, Hille, Neumcke, Nonner and Stämpfli (1976). The contributions of the different noise sources can be expressed in terms of a noise factor (F_t). The total density of the membrane current fluctuations (S_t) can be written as:

$$S_t = S_m + \frac{4kT}{R_m} F_t. \tag{5}$$

S_m represents the excess membrane noise, R_m is the membrane chord resistance and we assume that the thermal noise level of the membrane under nonequilibrium conditions is equal to $4kT/R_m$. Ideally, F_t will be equal to 1. In practice F_t is, however, far removed from this value. In the calculation of F_t at the holding potential we represent the membrane as an RC-system, where the $I-V$ curve is approximately linear. The resistive part of the membrane impedance in the final expression of Conti *et al.* (1976) is then equal to R_m.

After rearrangement of the terms in this expression and neglecting axoplasm and seal capacitances, the total noise factor can be expressed as follows:

$$F_t = F_{DC} F_{BC} F_{ED} \{F_a^0 + (2\pi f\tau)^2 F_a^\infty\} \tag{6}$$

where F_{DC}, F_{BC}, and F_{ED} are the noise factors of axoplasm DC, seal BC and axoplasm ED.

$$F_{DC} = 1 + \frac{R_{DC}}{R_M // R_{ED}} \tag{7}$$

$$F_{ED} = 1 + \frac{R_m}{R_{ED}} \tag{8}$$

$$F_{BC} = 1 + \frac{R_{DC} + R_m // R_{ED}}{R_{BC}}. \tag{9}$$

The noise factor of amplifier 1 is given by

$$F_a = 1 + \frac{R_{eq,v}}{R_g} + \frac{R_g}{R_{eq,i}}. \tag{10}$$

Table 1. Axoplasm resistance measurements

Node	R_{ED}(meas.) ($10^6\,\Omega$)	R_{ED}(calc.) ($10^6\,\Omega$)	l_{ED} (10^{-3} m)	ϕ_i (10^{-6} m)	ρ_{ED} (Ωm $\times 10^{-2}$)	R_{DC}(meas.) ($10^6\,\Omega$)	R_{DC}(calc.) ($10^6\,\Omega$)	l_{DC} (10^{-3} m)	$\frac{R_{ED}/l_{ED}}{R_{DC}/l_{DC}}$
760227	30.9	10.0	1.34	13.7	340				
760401	35.7	9.0	0.96	12.2	435	35.7	11.8	1.25	1.30
760408	22.0	7.8	1.15	14.4	312				
760413	24.2	9.5	1.20	13.3	280	26.7	11.4	1.44	1.09
760428	25.4	14.5	1.40	9.3	123				
760730	30.0	13.5	1.25	11.4	245				
760804	23.8	14.2	1.10	10.4	184	30.0	16.2	1.25	0.90
760805	26.2	13.6	1.44	12.2	213	23.8	11.8	1.25	0.96
760810	18.8	7.1	1.06	14.4	289	37.5	9.1	1.34	0.63
760826	21.3	9.5	1.17	13.1	312	32.5	11.5	1.41	0.79
760903	26.2	8.6	1.29	14.5	335				
760909	25.0	10.9	1.22	12.5	252	37.5	15.7	1.75	0.96
760914	18.8	8.1	1.37	15.4	256	15.0	8.5	1.44	1.32
761007	37.8	13.8	1.37	11.8	302	51.2	19.9	1.98	1.07
761013	22.5	9.8	1.25	13.4	323				
761109	22.2	9.0	1.06	12.8	270				
761217	23.3	9.3	1.12	13.0	276	30.8	11.9	1.44	0.97
761223	16.8	7.3	1.22	15.2	250				
770122	18.7	8.9	1.15	13.4	229				
770125	22.5	6.5	1.20	16.1	382	25.0	7.4	1.37	1.03
770127	15.0	8.0	1.30	15.1	207	20.0	10.2	1.66	0.95
770204	30.0	9.2	1.14	13.2	360	42.5	10.8	1.34	0.83
770505	22.0	15.5	0.94	9.2	156	42.0	29.8	1.80	1.00
770524	47.5	12.3	1.08	11.1	426				
770526	17.5	9.7	1.10	12.6	198				
Mean:	25.0	10.2	1.20	13.0	278	32.2	13.3	1.48	0.99
SD:	7.3	2.6	0.13	1.8	78	9.8	5.8	0.23	0.18

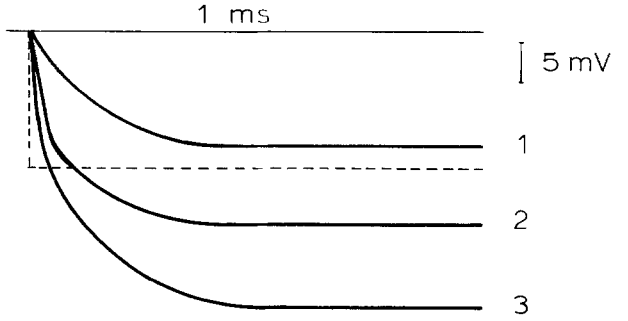

Fig. 3. Measurement of the electrical resistances of the nerve fiber. Voltage responses on current steps in pool *E* or *C* in the presence of feedback-isolation. Records fed through high-pass filter (*RC*-response, cutoff freq. of 2 Hz). Node 780114. *Curve 1:* output voltage of ampl. 1 on current step in pool *E*. *Curve 2:* output voltage of ampl. 2 on current step in pool *E*. *Curve 3:* output voltage of ampl. 1 on current step in pool *C*. The dashed line is the voltage response of a resistor of 50.6 MΩ, located close to the input terminal of amplifier 2. The curves yield the following resistances: 1: R_m; 2: $R_m + R_{ED}$; 3: $R_m + R_{DC}$

In these formulas // denotes a parallel arrangement. $R_{eq,v}$ is the equivalent resistance of the amplifier noise voltage and $R_{eq,i}$ is the equivalent resistance of the amplifier noise current. R_g (the source resistance at the amplifier's input) has a different value at low (^{0}) and high (^{00}) frequencies due to the shunting effect of membrane capacitance:

$$R_g^0 = R_{BC}//(R_{DC} + R_m//R_{ED}), \tag{11}$$

$$R_g^\infty = R_{BC}//R_{DC}. \tag{12}$$

The noise factor F_t increases at high frequencies due to the action of the membrane capacitance. The corner frequency is determined by the time constant τ:

$$\tau^2 = \{R_m//R_{ED}//R_{DC}\}\{R_m//R_{ED}//(R_{BC} + R_{DC})\}\, C_m^2. \tag{13}$$

The analysis of background noise by means of the noise factor gives a clear insight in the contributions of the different parts of the voltage-clamp configuration.

Results

Axoplasm Resistance Measurements

Axoplasm resistances were determined from the voltage responses to an applied current pulse in either pool *E* or in pool *C*. The differences between the output voltages of amplifiers 1 and 2 (Fig. 3) yield the axoplasm resistance R_{ED} or R_{DC}. In Table 1 these results are summarized together with the fiber geometry.

Table 2. Slow variations of the electrical resistances of the fiber

Preparation	t=0 hr R_{ED} ($10^6\,\Omega$)	t=1.5 hr R_{ED} ($10^6\,\Omega$)	t=0 hr R_{DC} ($10^6\,\Omega$)	t=1.5 hr R_{DC} ($10^6\,\Omega$)	t=0 hr R_{BC} ($10^6\,\Omega$)	t=1.5 hr R_{BC} ($10^6\,\Omega$)	t=0 hr R_{EF} ($10^6\,\Omega$)	t=1.5 hr R_{EF} ($10^6\,\Omega$)
760903	26.2	20.0	–	–	–	–	–	–
760909	25.0	12.5	–	–	–	–	–	–
761013	22.5	12.5	30.0	23.8	–	–	–	–
770525	47.5	31.2	40.0	33.7	47.7	780	36.0	26.9
770526	17.5	12.5	32.5	25.0	19.8	196	7.2	2.8
770531	32.5	21.2	50.0	41.2	15.6	13.8	5.6	2.7
770616	18.8	17.5	45.0	70.0	8.4	253	2.7	2.7
770712	25.0	12.5	50.0	37.5	25.0	825	15.2	4.0
770714	22.5	17.5	27.5	40.0	32.8	273	5.1	4.1
770802	20.0	16.3	33.8	41.2	43.8	45.3	4.9	8.1
770811	17.5	10.0	45.0	47.5	114.8	225	9.2	4.2
770913	25.0	22.5	36.3	40.0	16.2	148.1	17.5	4.0
770922	17.5	12.5	30.0	35.0	12.5	21.0	4.2	1.3
770923	42.5	32.5	42.5	75.0	19.3	193	5.0	2.6
770927	37.5	27.5	62.5	47.5	21.9	11.3	5.4	4.0
Mean:	26.5	18.6	40.4	42.9	46.3	249	9.8	5.6
761007	37.8	40.2	51.2	63.0	–	–	–	–
761109	22.2	30.0	–	–	–	–	–	–
761217	23.3	25.0	30.8	33.3	–	–	–	–
770125	22.5	23.7	25.0	25.0	16.7	58.2	–	–
770127	15.0	25.0	20.0	31.3	18.2	28.0	–	–
770816	30.0	50.0	37.5	90.0	88.6	215.6	10.3	1.3
770920	15.0	16.3	25.0	42.5	18.2	132.8	–	–
Mean:	23.7	30.0	31.6	47.5	35.4	108.7	–	–

Axoplasm Resistance and Calculation from Fiber Geometry

In Table 1 the measured resistance values are compared with the values predicted by Eq. (2) with the use of the assumed axoplasm resistivity of 110 Ω cm. There is a pronounced difference between the measured ($R_{\text{meas.}}$) and calculated ($R_{\text{calc.}}$) axonal resistance values under our experimental conditions. The mean ratio of $R_{\text{meas.}}$ and $R_{\text{calc.}}$ is 2.5. This factor lies far beyond the magnitude of the errors in the resistance measurements. For a number of fibers we calculated the ratio of the unit length resistances R_{ED}/l_{ED} and R_{DC}/l_{DC} (Table 1). The mean value of this ratio is close to 1. We conclude that the resistance of the axoplasm is indeed proportional to its length. The proportionality between R_{ED}/l_{ED} and $1/\phi_i^2$ could not be tested with the required accuracy, since the range of ϕ_i-values is small and its relative error too large.

Since silicone seals may deform the axon the application of Eq. (2) yields an apparent specific resistance, which equals to $278 \pm 78\,\Omega$ cm.

Slow Variations of the Axoplasm Resistances

The resistance values of the internodes and seals measured at the beginning and at the end of the experiment (time interval: 1.5 hr) show a marked difference (Table 2). In 68 % of the fibers (n=22) R_{ED} decreases 30 % of its original value (upper column). In the remaining fibers R_{ED} increases 27 % (lower column). On the average, R_{ED} decreases by 12 % (n=22), where R_{DC} increases by 18 % (n=19) of the original value. The seal R_{BC} increases 6 times (n=16) and the seal R_{EF} decreases to half its original value (n=13). This suggests an increase of the insulation by the oil-gap during the experiment, contrary to the silicone seal insulation.

Since no measurements were performed in between the start and the end of an experiment, information on the time course of the resistance variations was not obtained.

Ionic Current Parameters

With our membrane current measurement, we determined a number of ionic current parameters: $\bar{g}_L$, E_L, $\overline{g_K}$, E_K and maximum peak sodium current (Table 3). The peak inward current reaches its maximum close to −10 mV membrane voltage. With the leakage current parameters and measured potassium current (after addition of TTX) the maximum peak sodium current was found to be -16.33 ± 2.81 nA

Table 3. Ionic current parameters

Node	$I_{Na,\,max.\,peak}$ (10^{-9} A)	$\overline{g_L}$ (10^{-8} S)	E_L (mV)	$\overline{g_K}$ (10^{-8} S)	E_K (mV)	R_{ED} ($10^6\,\Omega$)	hp (mV)
770122	−17.35	1.82	−70	6.43	−75	18.7	−70.0
770802	−16.53	1.90	−45	4.00	−70	20.0	−70.0
770913	−18.60	2.67	−55	5.10	−74	25.0	−62.0
770922	−13.83	1.40	−65	7.46	−78	7.5	−70.0
770923	−16.10	1.33	−60	4.68	−68	43.5	−70.0
771103	−21.85	1.90	−60	9.50	−70	22.5	−68.0
771117	−12.01	1.90	−53	3.93	−76	17.5	−75.0
771124	−14.96	1.20	−75	7.65	−75	22.5	−80.0
771215	−13.10	1.25	−68	8.57	−58	24.4	−78.0
780107	−16.87	2.20	−60	9.31	−63	26.3	−64.0
780119	−18.37	1.28	−60	–	–	–	−68.0
Mean:	−16.33	1.71	−61	6.66	−71	22.8	−70.5
SD:	2.81	0.47	8.4	2.14	6.3	7.8	5.4

Table 4. Calculated noise factors at holding potential

Node	hp (mV)	R_m ($10^6\,\Omega$)	R_{DC} ($10^6\,\Omega$)	R_{BC} ($10^6\,\Omega$)	R_{ED} ($10^6\,\Omega$)	F_{DC}	F_{BC}	F_{ED}	F_a	F_t
780105 (R)	−80	91.7	26.3	89	16.3	2.90	1.45	6.63	1.13	32
771103 (TTXR)	−68	52.6	25.0	7.4	22.5	2.59	6.51	3.34	1.04	59
771110 (R)	−79	58.8	44.3	5.6	13.8	4.97	10.89	5.26	1.04	296
771117 (TTXR)	−75	52.6	25.0	7.3	17.5	2.90	6.22	4.01	1.04	75
771124 (R)	−80	83.3	55.0	36.4	22.5	4.10	3.00	4.70	1.11	64
771201 (R)	−78	58.8	35.0	300	27.5	2.87	1.18	3.14	1.21	13
771208 (TTXR)	−78	90.9	30.0	42.9	20.0	2.83	2.08	5.55	1.11	36
771222 (TTXR)	−78	75.8	26.3	16.4	16.3	2.96	3.42	5.65	1.06	61
Mean:	−77	70.6	33.4	63.1	19.6	3.27	4.34	4.79	1.09	79.5

(when the pulse to −10 mV was preceded by a negative pulse of −100 mV, with a duration of 40 msec). With the empirical formula's for the Hodgkin-Huxley rate constants of the sodium system, according to Conti et al. (1976) and $E_{Na} = +50$ mV, the maximal peak sodium current corresponds to a sodium permeability $\bar{P}_{Na}$ per node of 2.45×10^{-9} cm^3 sec^{-1} or to a sodium conductance at 0 mV $\overline{g_{Na,\,0}}$ of 49.6×10^{-8} S.

Membrane Current Fluctuations

Calculation of the background noise is possible because the noise factors F_{DC}, F_{BC}, F_{ED} and F_a contain quantities, which can be measured directly in this arrangement. In Table 4 the noise factors are calculated at the holding potential for low frequencies (1–500 Hz) neglecting the influence of capacitances. At these frequencies the amplifier noise factor lies close to unity, and most of the extraneous noise arises from the silicone seal *BC* and the axoplasm parts *DC* and *ED*. Due to the large variations in the values of R_{BC} in different preparations, F_{BC} is highly variable and thus the total noise factor F_t.

Noise current measurements on both nerve equivalent circuits and nerve fiber preparations are shown in Figs. 4 and 5. There is an excellent agree-

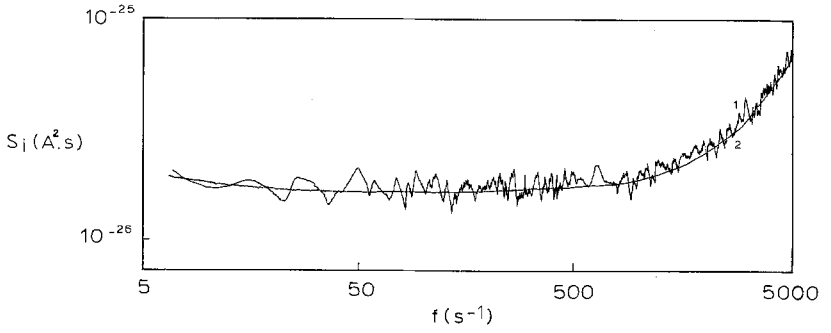

Fig. 4. Spectral density of the noise currents of a nerve equivalent circuit: $R_m = 48.6$ MΩ, $R_{DC} = 48.6$ MΩ, $R_{ED} = 24.8$ MΩ, $R_{BC} = 21.5$ MΩ and $C_m = 3.2$ pF. Curve 1 is the measured noise spectrum. The calculated background noise spectrum is shown in curve 2. Spectral density obtained according to the procedures outlined in Bendat and Piersol (1971). The amplitude variance error is 10 %. From 5–500 Hz the spectral resolution is 1.6 Hz and from 500–5000 Hz it is 6.7 Hz

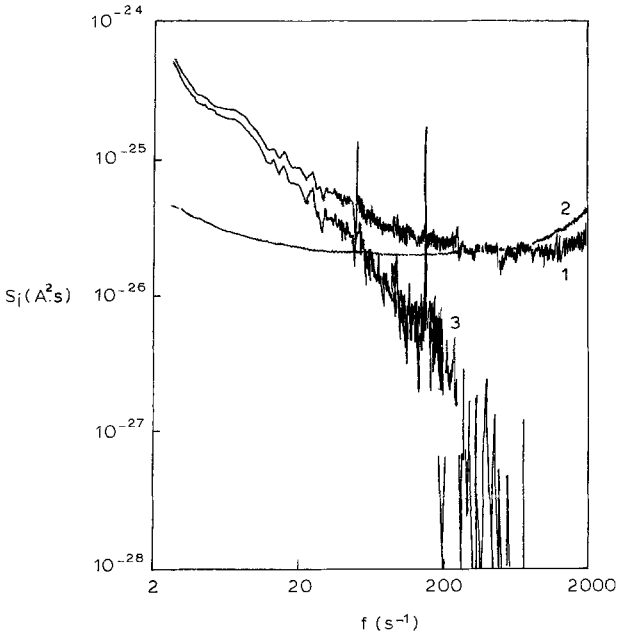

Fig. 5. Spectral density of the noise currents of the nerve membrane clamped at −60 mV in standard Ringer's solution (curve 1). Curve 2 represents the calculated background noise level. The difference between 1 and 2 (curve 3) is the excess noise intensity, which is of the 1/f-type. Deviation at higher frequencies is due to overestimation of the membrane capacitance. (Variance error is 10%. The spectral resolution changes from 0.67 Hz in the frequency range 2–200 Hz to 6.7 Hz in the range 200–2000 Hz)

ment between measured and calculated noise levels. At frequencies exceeding 1000 Hz a deviation of calculated and measured noise levels becomes significant. The discrepancy proved to be due to an inaccurate estimation of the membrane capacitance.

Discussion

Membrane Current Calibration Approaches

Determination of $R_{ED}(Z)$ is the key for current calibration in most voltage-clamp configurations for *Ranvier* nodes. Approaches 1 and 2 will be correct as far as the order of magnitude of the membrane current is considered. Calibration by approach 3 is shown to be correct only in case of a single seal of 100 µm (Schwarz, Neumcke & Stämpfli, 1979). Any changes in the internodal resistance cannot be detected. The same disadvantage appears in approach 5, where resistances can be calculated only after destruction of the nodal membrane. Approaches 4 and 6 differ in the directness of the measurement and allow R_{ED} determination at any time. With approach 6, R_{ED} can be obtained simply and the measurement is easily repeatable.

A direct measurement method of the membrane current by an external resistor is applied by Mozhaev, Mozhaeva and Naumov (1970), but only for slow voltage clamping (5 mV/sec).

Axoplasm Resistivity ρ

Determination of ρ from Eq. (2) is only possible if the internode can be approximated as a homogeneous cylinder. Since silicone seals may compress the nerve fiber an apparent ρ will be obtained, which is too large. The results of Schwarz et al. (1979) for a short seal point to a value of ρ of 110 Ω cm, as found indirectly by Huxley and Stämpfli (1951). With more seals the apparent value of ρ increases. With approach 4 Chiu et al. (1979) found a ρ of 158 Ω cm (single seal). Our value of 278 Ω cm obtained for two seals is probably the result of fiber constrictions.

Slow Variations in Axoplasmic Resistance

Addition of proteins and carbohydrates in ionic solutions leads to an increase of their resistivities (Carpenter, Hovey & Bak, 1973). Since the cut ends of the nerve fiber are bathed in a 120 mM KCl-solution, such substances will diffuse out of the axoplasm resulting in a lower resistivity. The slow increase of the axoplasm resistance can be due to continuing compression of the fiber by the seals or to partial resealing of the cut end.

The decrease of R_{ED} causes a decrease of the clamp amplifier output in pool *E*. This can be interpreted as a decrease of the ionic current. Assuming an exponential time course between the start and the end of the experiment the half-time of the R_{ED} decay amounts to 2.8 hr; for a linear decline this is 2.4 hr. In motor fibers the half-time for sodium and potassium current rundown is 1.5 and 0.7 hr.[4] Therefore a part of the rundown process may arise from the decline of axoplasm resistance.

Ionic Current Parameters.

Differences in ionic conductances of nodes under similar conditions between different laboratories may arise from differences in frog species, nodal membrane area and current calibration procedure.

The $\overline{P_{Na}}$ obtained by Dodge (1963) for *Rana pipiens*[5] (approach 2) is a factor 1.6 higher than our value. The ratio of Dodge's $\overline{g_K}$-values[6] and ours is

[4] Table 1 from Keana and Stämpfli (1974).

[5] $\overline{P_{Na}} = 4.0 \times 10^{-9}$ cm^3 sec^{-1}: mean value of 5 nodes (nodes 4, 7, 8, 11*c* and 12).

[6] $\overline{g_K} = 12.2 \times 10^{-8}$ S: mean value of 6 nodes (nodes 4, 7, 8, 11*c*, 12 and 15).

1.8, while the ratio of the leakage conductances is 1.5. This suggests that the differences are caused by the calibration procedure.

For *Rana esculenta* Conti et al. (1976) obtained a maximum peak sodium current of -31.38 nA (approach 3). The ratio of their sodium peak current and our peak current is 1.9. However, the ratio of the membrane resistance R_m at resting potential from their work and our values is 1.1–1.3. It remains unclear where this difference originates. By approach 4 Chiu et al. (1979) obtained a $\overline{g_{\mathrm{Na},0}}$ of 36×10^{-8} S, which is in the range of our value (50×10^{-8} S). However, their $\overline{g_L}$ of 3.7×10^{-8} S seems to be quite large. Sigworth (1980, approach 5) found $\overline{g_{\mathrm{Na},0}}$ to be 20×10^{-8} S and a $\overline{g_L}$ of 1.1×10^{-8} S.

To eliminate scaling differences introduced by nodal surface and axoplasm resistance we can compare the different $\overline{g_L}/\overline{g_{\mathrm{Na},0}}$ ratios obtained by approaches 3 through 6: 0.02 (Conti et al., 1976), 0.10 (Chiu et al., 1979) 0.06 (Sigworth, 1980) and 0.03 (this paper).

The leakage potential of the nodal membrane is found to be -61 ± 8 mV. No other direct measurements of the leakage equilibrium potential in the node exist. Dodge (1963) summarized arguments that the leakage is primarily carried by potassium ions and assigned $E_L=E_{\mathrm{K}}$. From our measurements we conclude that E_{K} is definitely more negative than E_L in standard Ringer's solution. The values of E_{K} probably have to be corrected for K^+-accumulation in the perinodal space. Therefore, the E_{K} is a lower limit. Errors in the determination of E_L may be introduced by contribution of K^+-current and ionic accumulation or depletion. Negative prepulses and negative test pulses (up to -200 mV) reduce I_{K} practically to zero. The magnitude of I_L is relatively small (maximal $\simeq2$ nA) and therefore ionic accumulation and/or depletion will probably not influence the measurements of E_L.

The knowledge of the reversal potential allows us to calculate the permeability ratio of cations in the leak. Neglecting the permeability of anions, and divalent cations it follows from the Goldman-Hodgkin-Katz equation that the permeability ratio $P_{\mathrm{Na}}/P_{\mathrm{K}}$ in the leak is 0.06.

Background Noise Calculation

With the analysis of noise factors one can easily judge which parts of the configuration dominate in the background noise spectrum. For a complete calculation at positive membrane potentials the small signal impedance of the node has to be measured.

The authors are grateful to Wim Deegenaars and Arie de Vos who were responsible for the design and maintenance of the electronic equipment. We also acknowledge the assistance of Ton Barhorst and Pedro Tetteroo in the computations of the background noise. This work is supported by the Netherlands Organization for the advancement of Pure Research (ZWO).

References

Bendat, J.S., Piersol, A.G. 1971. Random Data: Analysis and Measurement Procedures. Wiley-Interscience, New York

Carpenter, D.O., Hovey, M.M., Bak, A.F. 1973. Measurements of intracellular conductivity in *Aplysia* neurons: Evidence for organization of water and ions. *Ann. N.Y. Acad. Sci.* **204**:502

Chiu, S.Y., Ritchie, J.M., Rogart, R.B., Stagg, D. 1979. A quantitative description of membrane currents in rabbit myelinated nerve. *J. Physiol.* **292**:149

Conti, F., Hille, B., Neumcke, B., Nonner, W., Stämpfli, R. 1976. Measurement of the conductance of the sodium channel from current fluctuations at the node of Ranvier. *J. Physiol.* **262**:699

Derksen, H.E. 1965. Axom Membrane Voltage Fluctuations, Ph.D. Thesis, State University, Leiden. *See also: Acta Physiol. Pharmacol. Neerl.* **13**:373

Dodge, F.A., Frankenhaeuser, B. 1958. Membrane currents in isolated frog nerve fibre under voltage clamp conditions. *J. Physiol. (London)* **143**:76

Dodge, F.A. 1963. A Study of Ionic Permeability Changes Underlying Excitation in Myelinated Nerve Fibres of the Frog. Ph. D. Thesis, The Rockefeller University, N.Y. (*see* University Microfilms, Inc., Ann. Arbor, Mich., No. 64-7333)

Hille, B. 1971. The permeability of the sodium channel to organic cations in myelinated nerve. *J. Gen. Physiol.* **58**:599

Huxley, A.F., Stämpfli, R. 1951. Direct determination of membrane resting potential and action potential in single myelinated nerve fibres. *J. Physiol. (London)* **112**:476

Keana, J.F.W., Stämpfli, R. 1974. Effect of several "specific" chemical reagents on the Na^+, K^+ and leakage currents in voltage-clamped single nodes of Ranvier. *Biochim. Biophys. Acta* **373**:18

Moore, J.W., Del Castillo, J. 1959. An electronic electrode. IRE *Nat. Conv. Rec.* Pt. **9**:47

Mozhaev, G.A., Mozhaeva, G.N., Naumov, A.P. 1970. The influence of ions on steady-state potassium conductance of the Ranvier node membrane. *Tsitologiya*, **12, 8**:993

Nonner, W. 1969. A new voltage clamp method for *Ranvier* nodes. *Pfluegers Arch.* **309**:176

Nonner, W., Rojas, E., Stämpfli, R. 1975. Displacement currents in the node of *Ranvier*. Voltage and time dependence. *Pfluegers Arch.* **354**:1

Schwarz, W., Neumcke, B., Stämpfli, R. 1979. Longitudinal resistance of axoplasm in myelinated nerve fibres of the frog. *Pfluegers Arch.* **379**: R 41

Sigworth, F.J., 1980. The variance of sodium current fluctuations at the node of *Ranvier*. *J. Physiol. (London) (In press)*

Stämpfli, R. 1969. Dissection of single nerve fibres and measurement of membrane potential changes of *Ranvier* nodes by means of the double air gap method. *In:* Laboratory Techniques in Membrane Biophysics. H. Passow and R. Stämpfli, editors. p. 157. Springer-Verlag, New York

Tasaki, I. 1955. New measurements of the capacity and the resistance of the myelin sheath and the nodal membrane of the isolated frog nerve fibre. *Am. J. Physiol.* **181**:639

Van den Berg, R.J. 1978. Electrical fluctuations in Myelinated Nerve Membrane. A Source of Information. Ph. D. Thesis, State University, Leiden. (*See* University Library, Leiden)

Received 17 December 1979; revised 23 May 1980